PROCEEDINGS OF SCIENCE

Tracking the confinement phase transition in the thermodynamic observables of QCD at finite density

Yi Lu,[a,*] **Fei Gao,**[b] **Baochi Fu,**[c] **Huichao Song**[a,d,e] **and Yu-xin Liu**[a,d,e]

[a] *Department of Physics and State Key Laboratory of Nuclear Physics and Technology, Peking University, Beijing 100871, China*

[b] *School of Physics, Beijing Institute of Technology, Beijing 100081, China*

[c] *Fakultät für Physik, Universität Bielefeld, D-33615 Bielefeld, Germany*

[d] *Center for High Energy Physics, Peking University, Beijing 100871, China*

[e] *Collaborative Innovation Center of Quantum Matter, Beijing 100871, China.*

E-mail: qwertylou@pku.edu.cn

It is exciting that the heavy-ion collision experiments are now entering the high baryon density region in the QCD phase diagram, with an increasing number of high-statistics measurements expected in the near future. In this proceeding, we discuss possible signatures of QCD confinement at high density in two specific thermodynamic observables: the isentropic trajectories, and the baryon number fluctuations. For predicting the thermodynamic properties of these observables, new theoretical frameworks are developed for a direct calculation on the QCD equation of state via continuum correlation functions, especially for the confinement aspect via the Polyakov loops and the gluonic background field, which can be useful to tackle the urgently needed high density region, in parallel to experimental studies.

The XVIth Quark Confinement and the Hadron Spectrum Conference (QCHSC24)
19-24 August, 2024
Cairns Convention Centre, Cairns, Queensland, Australia

∗Speaker

ISSN 1824-8039. Published by SISSA Medialab.

PoS(QCHSC24)063

1. Introduction

With new facilities established, heavy-ion collision experiments are now entering the high baryon density region, where interesting physics phenomena such as the QCD critical end-point (CEP) and possible new phases are expected [1–3]. Correspondingly, an increasing amount of measurements and high-statistics data for the high density nuclear matter will come in the near future. In order to explain the phenomena in the observations and extract possible signals of new physics, there is a urgent need for theoretical analysis with precision at high baryon density in parallel. The key of such a combined study is to connect theory and experiment through specific thermodynamic observables. Typically, there are various observables discovered which shed lights on the chiral phase transition, see e.g. [4–6] for reviews. Yet, the confinement aspect, including the interplay between confinement and chiral symmetry, is much less understood, and its experimental signature is not quite clear. In this proceeding, we will show some recent progress on this at finite density, and highlight two thermodynamic observables that are characteristic to the confinement phase transition: the isentropic trajectories, and the baryon number fluctuations.

2. Phenomenology in the isentropic trajectories

The isentropic trajectories are the evolution trajectories of the system, along which the total entropy (S) of the system stays constant. For strong interaction matter where the net-baryon number N_B is conserved, one can further rewrite the isentropic condition as: $s/n_B = S/N_B = const$, with s and n_B the entropy and the net-baryon densities, respectively. In a recent work, we demonstrate that the thermodynamic properties encoded in the QCD isentropic trajectories, can be well captured via a refined QCD effective model which includes confinement phenomenology [7]. The key points of this model are summarised as follows.

2.1 Confinement via a refined effective model

Traditionally, the mean-field effective models start from constructing a model for the effective action Γ, then the quantum equation of motion (EoM) is qualitatively captured by a series of order parameters O:

$$\frac{\partial \Gamma[O]}{\partial O} = 0. \tag{1}$$

For QCD, some common choices are the quark condensate $O_\chi = \langle \bar{q}q \rangle$ and the Polyakov loop $O_{\text{conf.}} = \mathcal{L}$, which correspond to the chiral phase transition and the confinement-deconfinement transition, respectively. In principle, (1) determines all properties of the system, including the correlation functions. Take the quark propagator G_q for example, in the momentum space it follows:

$$[G_q^O(\boldsymbol{p}, \omega_n)]^{-1} \approx \mathrm{i}(\omega_n + \mathrm{i}\mu_q - gA_0[O_{\text{conf.}}])\gamma_0 + \mathrm{i}\boldsymbol{\gamma} \cdot \boldsymbol{p} + M_q[O_\chi]. \tag{2}$$

As a price to pay in the mean-field models, the mass function M_q is momentum-independent, i.e. it does not carry the specific dynamics of the strong interaction.

Alternatively, one can also start directly from modeling the correlation functions, and this is what we have explored recently. As a preliminary attempt, we still consider the form in (2) for simplicity and focus on its thermodynamic properties. Then, we implement the T and μ_B

dependencies of the order parameters from calculations which incorporate the full quantum, thermal and density fluctuations. These dependencies are what the first-principles lattice QCD simulation, as well as functional QCD approaches and so on, can provide. Remarkably, functional QCD approaches provide a direct access at finite density, with converging results for the chiral order parameters towards the onset CEP location of QCD, see [8–10]. We then refer to these data as inputs.

The advantage of such a framework is that, one can establish a direct relation between the observables and the current-best knowledge on the order parameters, particularly the Polyakov loop $\mathcal{L}$. This can be seen in the net-quark number density n_q as a crucial thermodynamic observable:

$$n_q = -\mathrm{Tr}\,\gamma_0 G_q^O = \int \frac{d^3\boldsymbol{p}}{(2\pi)^3}\left[f_q^+(\boldsymbol{p},\mathcal{L}) - f_q^-(\boldsymbol{p},\mathcal{L})\right], \tag{3}$$

with $f_q^{+/-}$ the modified quark/anti-quark distribution functions being analytic to $\mathcal{L}$, see the details in [7]. As a consequence, we found that the underlying phase transition line:

$$T(\mu_B) \simeq T_c(0)\left[1 - \kappa_2\left(\frac{\mu_B}{T_c(0)}\right)^2\right], \tag{4}$$

offers a way for further simplifications of the data inputs in (3). Specifically, one can further parameterise the order parameter data according to (4) and using the T' expansion [11]:

$$\mathcal{L}(T,\mu_B) \simeq \mathcal{L}_{\mathrm{data}}(T'(T,\mu_B),0), \tag{5}$$

$$T' = T(1+\kappa(\mu_B/T)^2+\cdots), \tag{6}$$

then at small μ_B, such parameterisations can offer the same precision level as a direct input of data. However, towards higher μ_B, the phenomenology of CEP has to be further included. We accomplish this by referring to the up-to-date estimate of the CEP location $\mu_B^{\mathrm{CEP}} \approx 600\,\mathrm{MeV}$ [8–10], and then combining (4) with the Ising parameterisation form [12, 13] for the order parameter.

2.2 Confinement signatures in the trajectories

The finite density contribution to QCD thermodynamic functions can be fully determined by the correlation function of matter sector (2), using the general thermodynamic relations:

$$P(T,\mu_B) = P(T,0) + \sum_q \int_0^{\mu_B} n_q(T,\mu)\,d\mu, \qquad s = \frac{\partial P}{\partial T}, \qquad \cdots. \tag{7}$$

The isentropic trajectories in QCD $s/n_B = const.$ can then be extracted, see our results for the finite μ_B region in the left column of Figure 1. It is interesting to notice that with a minimal treatment of (3), the obtained thermodynamic functions already agree well to the lattice QCD extrapolation [14] within the error bars, in the region of $\mu_B/T \lesssim 2$ where the lattice extrapolation still have a good control of convergence. However, there are still limitations in the framework, such as for the description of thermodynamic functions with high-order μ_B derivatives, please find the discussions in [7]. On the other hand, we observed that the trajectories shows clearly a bending behaviour from high to low temperatures, and the onset temperature of the bending is close to the phase boundary.

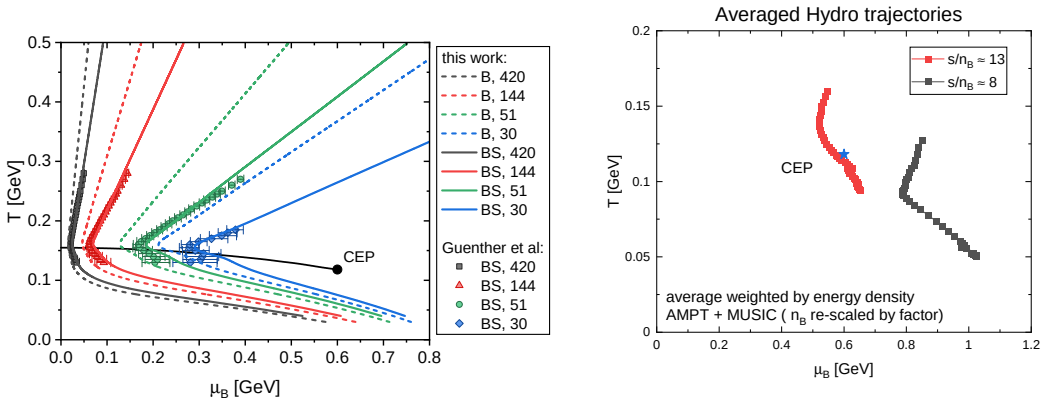

Figure 1: Left: QCD isentropic trajectories $s/n_B = const.$ in the 3-flavour degenerate case (B) and in the 2+1-flavour case with strangeness neutrality (BS); for the strangeness-neutral case, the lattice QCD result from [14] is displayed for comparison. Right: evolution trajectories for heavy-ion collision systems, predicted by combining the equilibrium equation of state with hydrodynamic simulation (MUSIC+AMPT).

We verified that by setting the Polyakov loop as the fully deconfined value $\mathcal{L} = 1$, the trajectories show a sizable difference to the ones in the left column of Figure 1, especially at low temperatures, and the bending feature can even disappear. This suggests that the bending of the trajectories has a phenomenological connection to the confinement phase transition.

We then further investigate the bending of the evolution trajectories in realistic systems. For heavy-ion collisions, we combine with the hydrodynamic simulation (MUSIC+AMPT) [15] and show that the observed bending behaviour in the trajectories remains unchanged, when the dynamical evolution of non-equilibrium effect is further included, see in the right column of Figure 1. As a by-product, we also give an estimate on the onset s/n_B value of the trajectory that crosses the CEP, which is $s/n_B \approx 13$. Preliminary estimate also shows that the trajectory bends sharply when crossing the first-order transition region, which indicates that the chiral and confinement aspects of QCD have strong overlaps near and above CEP. In fact, in the cosmological scenario, the critical lensing phenomenon is further observed in the cosmic trajectories close to the CEP [16], which may also be an outcome of such overlaps. Together, it indicates that the isentropic trajectory may serve as a universal observable for inspecting the change of relevant degrees of freedom in the high density system during a phase transition.

3. Self-consistent resolution of confinement and baryon number fluctuations

Microscopically, the dynamics of confinement and center symmetries is encoded in the gluon background field A_0, which is a 1-point correlation function in QCD. Such a correlation function is directly accessible at finite temperature and density using functional QCD approaches, including the Dyson-Schwinger equations (DSE) approach [17–19] and the functional renormalisation group (fRG) approach [10, 17, 20–22]. As a brief demonstration, the quantum EoM for A_0 in the DSE approach is shown diagrammatically as Figure 2. Its computation requires only the knowledge of full propagators and the full interaction vertices, marked as the solid grey blobs, which have been carefully studied in previous literatures [17, 18]. In fact, it was also shown that the 2-loop

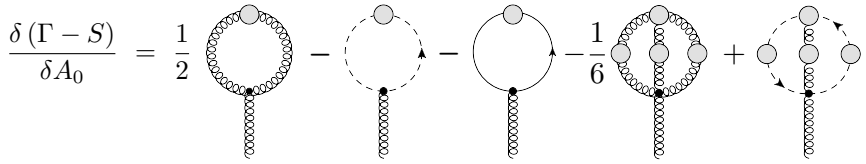

Figure 2: Diagrammatic description of the Dyson-Schwinger equations for the background field A_0.

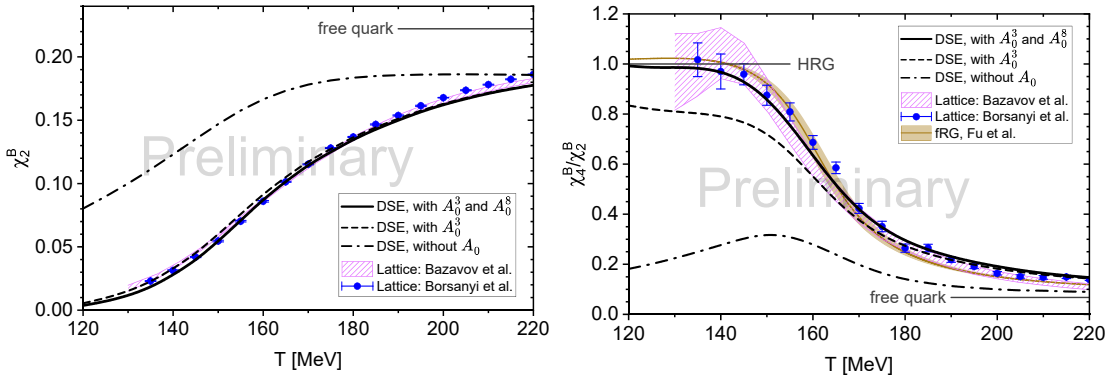

Figure 3: Baryon number fluctuations, including the second-order susceptibilities χ_2^B (left) and the kurtosis χ_4^B/χ_2^B (right) at zero chemical potentials. A comparison of the results with and without background field is shown for both A_0^3 and A_0^8 components. The corresponding results from hadron-resonance gas (HRG) model, lattice QCD [23, 24] and fRG [25] are also displayed.

contributions can be minimised by properly setting the renormalisation scale, see the analysis in [17]. This then enables further simplifications with the diagrammatic "one-loop" truncation and taking only the full propagators as inputs, see the applications in [18], which is also applied in our studies.

We then discovered that the gluon background A_0 can offer a unified solution on both the confinement-deconfinement phase transition, as well as QCD thermodynamic observables. The idea is to implement the A_0 solution from the quantum EoM in Figure 2 as a feedback into the matter sector, namely the full quark propagator G_q, which then offers a self-consistent determination on:

$$\text{chiral condensate:} \qquad \langle \bar{q}q \rangle = -T \sum_{n\in\mathbb{Z}} \int \frac{d^3\boldsymbol{p}}{(2\pi)^3} \mathrm{tr}\, G_q(\boldsymbol{p}, \tilde{\omega}_n - gA_0), \tag{8}$$

$$\text{net-number density:} \qquad \langle \bar{q}\gamma_0 q \rangle = -T \sum_{n\in\mathbb{Z}} \int \frac{d^3\boldsymbol{p}}{(2\pi)^3} \mathrm{tr}\, \gamma_0 G_q(\boldsymbol{p}, \tilde{\omega}_n - gA_0), \tag{9}$$

and so on, where the Matsubara frequencies $\tilde{\omega}_n = (2n+1)\pi T + \mathrm{i}\mu_q$.

By comparing (8) and (9) to the case without A_0 feedback, we identify that the density fluctuations, namely the μ_B susceptibilities of (9):

$$\chi_k^B = \frac{\partial^k (P/T^4)}{\partial(\mu_B/T)^k} = \frac{\partial^{k-1}(n_B/T^3)}{\partial(\mu_B/T)^{k-1}}, \quad k = 1, 2, \cdots, \tag{10}$$

are characteristic of the finite density signatures of confinement phase transition. The comparisons are given in Figure 3 for the second-order susceptibility χ_2^B and for the kurtosis χ_4^B/χ_2^B. Here, the propagators take inputs from a recent work on the QCD phase structure [26], in order to solve the DSEs in Figure 2. In addition, the full color SU(3) structure of A_0 is considered:

$$A_0 = A_0^3 t^3 + A_0^8 t^8, \tag{11}$$

since at finite chemical potentials, the Cartan t^8 component of A_0 takes generally a finite value [27]. In concrete, it is observed that at low temperatures, the A_0 feedback suppresses the value of second order susceptibility, while it gives an enhancement on the kurtosis. Both A_0^3 and A_0^8 components are crucial, regarding their contributions to high-order fluctuations, such as the kurtosis in the right column of Figure 3. With a full consideration of A_0 effect, we obtain the temperature dependence of the baryon number susceptibilities with precision, compared with the lattice QCD results with a high order of Taylor expansions [23, 24] and the fRG results [25] as benchmarks. Remarkably, it provides for the first time a qualitative reliable calculation of the kurtosis within the DSEs approach, considering its low temperature limit. Further applications are also available for this background field framework, such as the determination on the QCD equation of state at finite density, which may serve as a useful framework to tackle the in-demand high density region for predictions on QCD thermodynamics. A separate article will come up soon for the specific discussions in the near future.

4. Conclusion

With the continuum approaches of QCD, we have developed new frameworks for studying the dynamics of confinement at finite density. The starting point is the QCD correlation functions of the matter sector, typically the full quark propagator. Then, the aspect of confinement can be captured either by a direct input from its order parameter - Polyakov loop, or by a self-consistent resolution via the gluon background field A_0. We then demonstrated two possible observables which are characteristic to the confinement-deconfinement phase transition. One is the isentropic trajectories, which show a bending feature near the phase boundary. Such a bending feature is not altered for realistic QCD systems, and it might indicate an overlap between the chiral and the confinement aspect of QCD at high density. The other one is the baryon number fluctuation, where we demonstrated the contributions of different A_0 components and their connections to the confining regime in QCD. Remarkably, we have presented for the first time a qualitative reliable calculation of the kurtosis within the DSEs approach. Together, the present studies may offer new strategies for solving the QCD thermodynamics in the in-demand high density region.

5. Acknowledgements

We thank Isabel M. Oldengott and Jan M. Pawlowski for collaborations on related subjects. Yi Lu and Fei Gao also thank the other members of fQCD collaboration [28] for discussions. This work is supported by the National Natural Science Foundation of China under Grants No. 12247107, No. 12175007 and No. 12075007. Baochi Fu is also supported by the National Natural Science Foundation of China under Grants No. 12147173. Fei Gao is supported by the National Science Foundation of China under Grants No. 12305134.

References

[1] Jinhui Chen et al. Properties of the QCD matter: review of selected results from the relativistic heavy ion collider beam energy scan (RHIC BES) program. *Nucl. Sci. Tech.*, 35(12):214, 2024.

[2] Xiaohong Zhou and Jiancheng Yang. Status of the high-intensity heavy-ion accelerator facility in China. *AAPPS Bull.*, 32(1):35, 2022.

[3] Tetyana Galatyuk. Future facilities for high μ_B physics. *Nucl. Phys. A*, 982:163–169, 2019.

[4] Gert Aarts et al. Phase Transitions in Particle Physics: Results and Perspectives from Lattice Quantum Chromo-Dynamics. *Prog. Part. Nucl. Phys.*, 133:104070, 2023.

[5] Lipei Du, Agnieszka Sorensen, and Mikhail Stephanov. The QCD phase diagram and Beam Energy Scan physics: a theory overview. *Int. J. Mod. Phys. E*, 33(07):2430008, 2024.

[6] John W. Harris and Berndt Müller. "QGP Signatures" Revisited. *Eur. Phys. J. C*, 84(3):247, 2024.

[7] Yi Lu, Fei Gao, Baochi Fu, Huichao Song, and Yu-Xin Liu. Constructing the equation of state of QCD in a functional QCD based scheme. *Phys. Rev. D*, 109(11):114031, 2024.

[8] Fei Gao and Jan M. Pawlowski. Chiral phase structure and critical end point in QCD. *Phys. Lett. B*, 820:136584, 2021.

[9] Pascal J. Gunkel and Christian S. Fischer. Locating the critical endpoint of QCD: Mesonic backcoupling effects. *Phys. Rev. D*, 104(5):054022, 2021.

[10] Wei-jie Fu, Jan M. Pawlowski, and Fabian Rennecke. QCD phase structure at finite temperature and density. *Phys. Rev. D*, 101(5):054032, 2020.

[11] S. Borsányi, Z. Fodor, J. N. Guenther, R. Kara, S. D. Katz, P. Parotto, A. Pásztor, C. Ratti, and K. K. Szabó. Lattice QCD equation of state at finite chemical potential from an alternative expansion scheme. *Phys. Rev. Lett.*, 126(23):232001, 2021.

[12] Micheal Kahangirwe, Steffen A. Bass, Elena Bratkovskaya, Johannes Jahan, Pierre Moreau, Paolo Parotto, Damien Price, Claudia Ratti, Olga Soloveva, and Mikhail Stephanov. Finite density QCD equation of state: Critical point and lattice-based T' expansion. *Phys. Rev. D*, 109(9):094046, 2024.

[13] Jamie M. Karthein, Volker Koch, and Claudia Ratti. Description of the first order phase transition region of an equation of state for QCD with a critical point. *Phys. Rev. D*, 111(3):034013, 2025.

[14] J. N. Guenther, R. Bellwied, S. Borsanyi, Z. Fodor, S. D. Katz, A. Pasztor, C. Ratti, and K. K. Szabó. The QCD equation of state at finite density from analytical continuation. *Nucl. Phys. A*, 967:720–723, 2017.

[15] Baochi Fu, Kai Xu, Xu-Guang Huang, and Huichao Song. Hydrodynamic study of hyperon spin polarization in relativistic heavy ion collisions. *Phys. Rev. C*, 103(2):024903, 2021.

[16] Fei Gao, Julia Harz, Chandan Hati, Yi Lu, Isabel M. Oldengott, and Graham White. Baryogenesis and first-order QCD transition with gravitational waves from a large lepton asymmetry, arXiv:2407.17549.

[17] Leonard Fister and Jan M. Pawlowski. Confinement from Correlation Functions. *Phys. Rev. D*, 88:045010, 2013.

[18] Christian S. Fischer, Leonard Fister, Jan Luecker, and Jan M. Pawlowski. Polyakov loop potential at finite density. *Phys. Lett. B*, 732:273–277, 2014.

[19] Christian S. Fischer, Jan Luecker, and Jan M. Pawlowski. Phase structure of QCD for heavy quarks. *Phys. Rev. D*, 91(1):014024, 2015.

[20] Jens Braun, Holger Gies, and Jan M. Pawlowski. Quark Confinement from Color Confinement. *Phys. Lett. B*, 684:262–267, 2010.

[21] Jens Braun, Lisa M. Haas, Florian Marhauser, and Jan M. Pawlowski. Phase Structure of Two-Flavor QCD at Finite Chemical Potential. *Phys. Rev. Lett.*, 106:022002, 2011.

[22] Wei-jie Fu and Jan M. Pawlowski. Relevance of matter and glue dynamics for baryon number fluctuations. *Phys. Rev. D*, 92(11):116006, 2015.

[23] A. Bazavov et al. The QCD Equation of State to $O(\mu_B^6)$ from Lattice QCD. *Phys. Rev. D*, 95(5):054504, 2017.

[24] Szabolcs Borsanyi, Zoltan Fodor, Jana N. Guenther, Sandor K. Katz, Kalman K. Szabo, Attila Pasztor, Israel Portillo, and Claudia Ratti. Higher order fluctuations and correlations of conserved charges from lattice QCD. *JHEP*, 10:205, 2018.

[25] Wei-jie Fu, Xiaofeng Luo, Jan M. Pawlowski, Fabian Rennecke, Rui Wen, and Shi Yin. Hyper-order baryon number fluctuations at finite temperature and density. *Phys. Rev. D*, 104(9):094047, 2021.

[26] Yi Lu, Fei Gao, Yu-Xin Liu, and Jan M. Pawlowski. QCD equation of state and thermodynamic observables from computationally minimal Dyson-Schwinger equations. *Phys. Rev. D*, 110(1):014036, 2024.

[27] Urko Reinosa, Julien Serreau, and Matthieu Tissier. Perturbative study of the QCD phase diagram for heavy quarks at nonzero chemical potential. *Phys. Rev. D*, 92:025021, 2015.

[28] fQCD collaboration, 2024. J. Braun, Y.-r. Chen, W.-j. Fu, F. Gao, F. Ihssen, A. Geissel, C. Huang, Y. Lu, J. M. Pawlowski, F. Rennecke, F. Sattler, B. Schallmo, J. Stoll, Y.-y. Tan, S. Töpfel, J. Turnwald, R. Wen, J. Wessely, N. Wink, S. Yin, H.-w. Zheng and N. Zorbach.